

Performance evaluation of a combined HiperLAN/2-Bluetooth digital front-end

Lars van Mourik, Roel Schiphorst, Fokke Hoeksema and Kees Slump

University of Twente, Department of Electrical Engineering,
Laboratory of Signals and Systems,

P.O. box 217 - 7500 AE Enschede - The Netherlands

Phone: +31 53 489 2780 Fax: +31 53 489 1060

E-mail: {l.c.vanmourik,r.schiphorst,f.w.hoeksema,c.h.slump}@el.utwente.nl

Abstract— In our Software-Defined-Radio (SDR) project we aim to combine two receivers (HiperLAN/2 and Bluetooth) on one common platform. In this paper, the main focus is on one of the performance bottlenecks of such a receiver, namely the bandpass filter section in Bluetooth mode. Contributions of inter-symbol interference *ISI*, adjacent channel interference *ACI* and noise on the total bit error rate *BER* are analyzed. The influence of the channel selection filter characteristics on these contributions are researched. Larger values for (for instance) transition bandwidth result in lower order filters that reduce the computational load, which is an important design consideration. This also reduces bit errors caused by *ISI*, one of the two major contributors to the total *BER*. On the other hand, lower order filters increase the *BER* due to *ACI*. Optimal filter parameters are derived from these trade-offs and applied the system which will be presented.

I. INTRODUCTION TO THE SDR PROJECT

In our Software-Defined-Radio (SDR) project [4] we aim to combine two receivers (HiperLAN/2 and Bluetooth) on one common platform. Our focus is from antenna output to raw bits. In our opinion, SDR is an implementation technology which aims at providing flexibility and reconfigurability to hardware platforms. The HiperLAN/2 hardware is that complex compared to the Bluetooth hardware, that Bluetooth capability may be added to the HiperLAN/2 platform at limited costs. So, it is not the demand for flexibility (one front end for all signals) that motivates us, but the idea of providing added functionality nearly for free. We've built a test bed with two separate receivers (HiperLAN/2 and Bluetooth), partly in hardware (analog front end) and partly in software (digital front end). This paper will only focus on the digital channel selection part of these two receivers (shown in figure 1).

The analog front end of our demonstrator (described in [1]) includes two Analog to Digital Con-

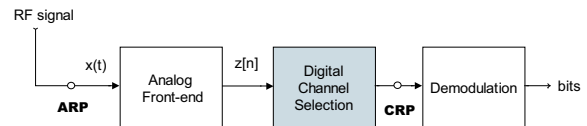


Fig. 1

THE SDR RECEIVER FUNCTIONAL BLOCKS

verters (ADCs) and produces a complex 80 MSPS signal $z[n]$ (see figure 1). For HiperLAN/2 the output is one channel at baseband (with a nominal bandwidth of 20 MHz) as our HiperLAN/2 demodulator requires a complex 20-MSPS baseband signal. On the other hand, for Bluetooth, the output of the analog front end is a "chunk" of 20 Bluetooth channels (with a nominal bandwidth B_{BT} of 1 MHz each)[2]. Our Bluetooth demodulator requires a real bandpass signal with center frequency located at 2.5 MHz (with 10 samples per symbol [5]). So the digital channel selection executes three functions: mixing (only Bluetooth), filtering and downconversion.

First an introduction will be given to the channel selection system of the receiver. Both HiperLAN/2 and Bluetooth modes will be described. Then, a more in-depth presentation is given of the Bluetooth channel selection requirements and design considerations. After discussing the *BER* calculation methods and trade-offs of the system, some experiments are defined to evaluate the system. After discussing the results, conclusions are drawn and final specifications of the current (test bed) system are given.

II. INTRODUCTION TO THE CHANNEL SELECTION SYSTEM

The current channel selection system operates in two different modes, depending on the input signal: HiperLAN/2 or Bluetooth. The input signal $z[n]$ (see

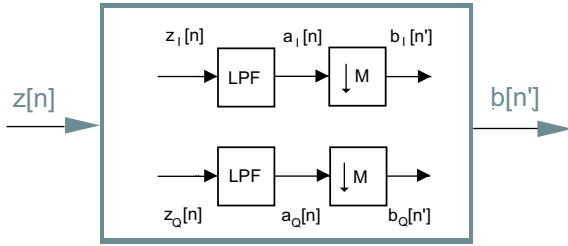


Fig. 2

HIPERLAN/2 DIGITAL CHANNEL SELECTION SYSTEM,
 $M = 4$

figure 1) originates from the AD converters, placed at the end of the analog front-end. The signal is complex for both modes and the sample-rates are also equal (80 MSPS). The output signal (of the channel selection system) however differs significantly for both modes. These differences are mainly imposed by demodulator requirements [7].

In HiperLAN/2 mode, the currently proposed configuration of the digital channel selection system is shown in figure 2. The complex input ($z_I[n], z_Q[n]$) is lowpass filtered (*LPF*) to remove adjacent HiperLAN/2 channels and other possible interferers. Then, decimation by a factor $M = 4$ is performed.

For Bluetooth mode, the configuration is shown in figure 3. Again, the complex input ($z_I[n], z_Q[n]$) is lowpass filtered (*LPF*) and decimated. Bluetooth inputs are decimated by a factor $M = 8$, which is done in two steps: $M = M1 \cdot M2 = 4 \cdot 2$. After the first decimation ($M1$), the resulting signals ($b_I[n'], b_Q[n']$) have a sample rate of 20 MSPS and contain 20 Bluetooth channels. Channels 0-9 are located in the lower sideband, which means that their carrier frequency $f_c < 0$ MHz. Thus, channels 10-19 are in the upper sideband and have carrier frequencies $f_c > 0$ MHz. A Hilbert transformer, implemented by a FIR filter is applied to the quadrature signal path ($b_Q[n']$). The in-phase signal $b_I[n']$ is delayed to compensate for the Hilbert transformer filter delay. Then, the phase shifted $c_Q[n']$ signal is *added to* or *subtracted from* $c_I[n']$. If the signals are subtracted, the resulting (real) signal $d[n']$ contains channels 0-9 (and of course: addition yields channels 10-19). This is the first step in the actual channel selection of the system.

The second step is performed by the first bandpass filter *BPF1*. The bandwidth of *BPF1* is defined as

B_1 . Assuming the Bluetooth Signal-Of-Interest (SOI) has a carrier frequency $f_c = 4.5$ MHz, the filter cut-off frequencies $f_{1,p}, f_{1,s}$ are defined as $f_c \pm B_1/2$. The resulting signal $e[n']$ is mixed with $f_{lo} = 2$ MHz. Output $f[n']$ now contains two images of the SOI at $f'_{c,1}, f'_{c,2} = 2.5, 6.5$ MHz. The *BPF2* filter removes the unwanted image with (in this case) $f'_{c,2} = 6.5$ MHz. After the second decimation by factor $M2 = 2$ the signal is ready for demodulation.

A. Bluetooth: requirements

The main objective of this design is to achieve the *BER*, required under well defined circumstances, with the least amount of computations. For Bluetooth, a maximum allowable *BER* is defined for certain worst case input scenarios [8]. This *BER* ($1 \cdot 10^{-3}$) will be calculated using simulations of over $3 \cdot 10^4$ bits. For a given demodulator, the *BER* performance is directly related to the signal-to-noise ratio (SNR_{demod}) of the signal [5]. SNR_{demod} depends on the received carrier power, analog filter bandwidth *B* and the received interference.

The received interference consists of the reception of one other Bluetooth signal. This interfering signal can have four different carrier frequencies ($f_{co}, f_{a,1}, f_{a,2}$ and $f_{a,3}$) and strengths (listed below, frequencies are given in MHz) [8]:

- f_{co} Co-channel interference with $f_{co} = f_c$
power is -11 dB relative to the SOI.
- $f_{a,1}$ First adjacent channel interferer (closest neighbor) with $f_{a,1} = f_c \pm 1$ MHz.
Signal power is equal to that of the SOI.
- $f_{a,2}$ Second adjacent channel interferer, at least 2 MHz away ($f_{a,2} = f_c \pm 2$ MHz).
This signal may be up to +30 dB stronger than the SOI.
- $f_{a,3}$ Third adjacent channel interferer, 3 or more MHz away ($f_{a,3} = f_c \pm k$ MHz, where $k \in [3, 4, 5, \dots]$). This interference may be up to +40 dB stronger.

These four input signals are also shown in figures 5(a-d). Of the $f_{a,3}$ category, only the most stringent ($k = 3$) is shown. In addition to these four interferers, each subplot also depicts the SOI, thermal noise (-37 dB relative to SOI) and the transfer function of the first bandpass filter (*BPF1*).

B. Bluetooth: eye diagrams and BER calculation

A Bluetooth signal is modulated using Gaussian Frequency Shift Keying (GFSK) [5]. This effectively

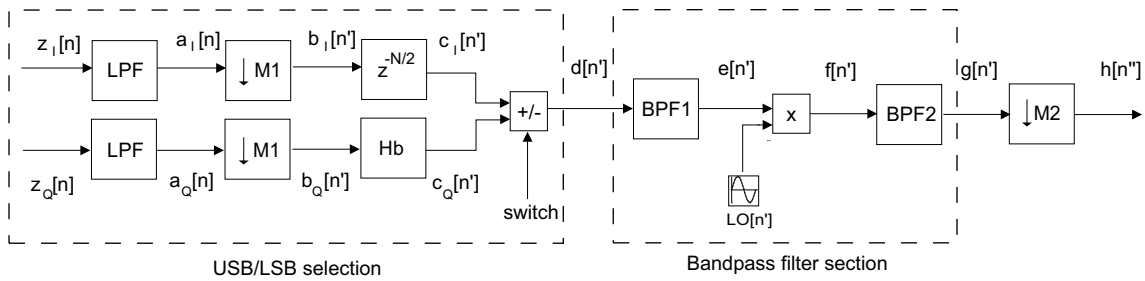


Fig. 3

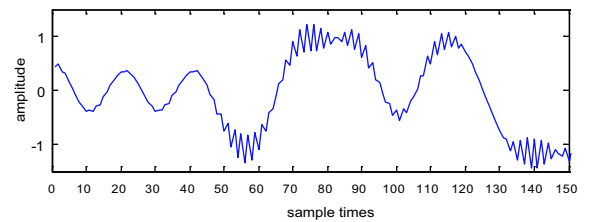
BLUETOOTH DIGITAL CHANNEL SELECTION SYSTEM, $M1 = 4, M2 = 2$

means that a transmitted "1" causes f_c to shift to $f_1 = f_c + f_{\Delta 1}$ and a transmitted "0" results in $f_0 = f_c - f_{\Delta 0}$. In our Bluetooth modulator $f_{\Delta 0} = f_{\Delta 1}$ and depends on the modulation index $h = 0.28 \dots 0.35$ (defined in [8]).

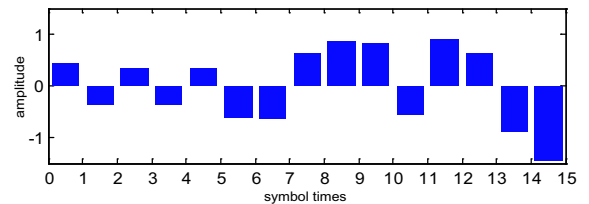
After decimation, channel selection filtering and mixing, the output signal ($h[n'']$) of the digital channel selection system is processed by a demodulator using an FM to AM conversion function $\mathbf{F}_{\text{FM} \rightarrow \text{AM}}(\cdot)$ [5]. The frequency variations are thus converted back to amplitude variations representing the received bits. Figure 4(a) depicts the converted output signal $\mathbf{F}_{\text{FM} \rightarrow \text{AM}}(\mathbf{h}[n''])$ of a fully processed input signal $z[n]$ with no interferers. Every 10 samples ($= T_{\text{symbol}} = T_{\text{bit}}$) a decision is made whether the transmitted bit was "0" or "1". In figure 4(b) the resulting (soft) bit sequence is shown. By choosing an appropriate trigger moment and plotting each symbol time T_s on top of the next, a so-called eye diagram is obtained (see figure 4(c)). The x-axis thus depicts 10 sample times, and the y-axis is the amplitude of a signal representing this bit. The eye diagram shows the decision moment that was chosen by the demodulator algorithm. The "open-ness" of the eye diagram will be referred to as $\Delta A_{0,1}$, defined as $\Delta A_{0,1} = A_1 - A_0$ (with A_0, A_1 as defined in figure 4(c)). The demodulated received bits are written to an output file to determine the *BER* by comparing them to the transmitted bits.

C. ACI vs ISI trade-off

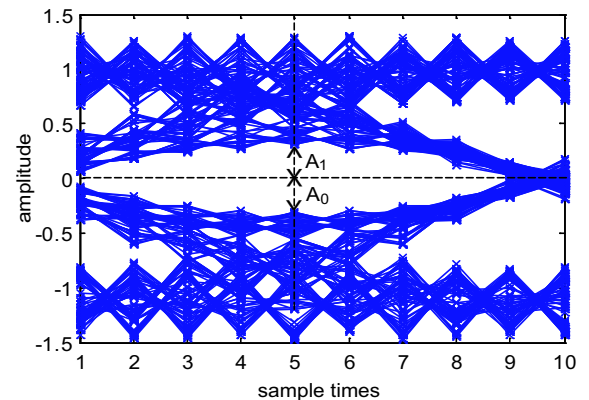
By introducing bandpass filters to the system (to remove adjacent channel interference and noise), intersymbol interference (*ISI*) is introduced to the system. Narrow bandpass filters increase *ISI*, which can be seen in the eye diagrams as narrowing $\Delta A_{0,1}$ (see figure 4(c)). Thus, the probability of correctly detecting whether a "0" or "1" was transmitted [3] is reduced because of narrow bandpass filters. The ef-



(a) Sample times (wave)



(b) Symbol times (soft bits)



(c) Eye diagram

Fig. 4

FM TO AM CONVERTED $h[n'']$ SIGNAL, NO INTERFERERS

fects of *ISI* are also clearly demonstrated in figures 4(a) and (b). The first 5 soft bits ($0 \leq t \leq 5 \cdot T_s$) are "10101" and each have an amplitude of ≈ 0.4 . The next 5 bits ($5 \cdot T_s \leq t \leq 10 \cdot T_s$) are "00111" and have significantly larger amplitudes. Thus, if for instance the "10101" amplitude variations become more and more dispersed by choosing a very narrow filter bandwidth, they can eventually cancel each other out. This relationship works two ways. To reduce bit errors caused by *ISI* (BER_{ISI}), the filter bandwidth can be *increased*. This leads to a reduction of channel selectivity and stronger interference from adjacent channels, increasing bit errors caused by *ACI* (BER_{ACI}). Thus, by reducing BER_{ISI} , BER_{ACI} is *increased*. The sensitivities of both contributions and resulting trade-offs will be analyzed in this paper.

III. SYSTEM ANALYSIS

The performance of the system under review depends mainly on sample rate, signal type (real or complex) and the number of filter coefficients used. The performance figure of the system (assessing computational complexity, as discussed in [7]) is minimized by using several methods. These include polyphase implementation of the filters, and length reduction (trade-offs) of filters operating at higher rates and the choice of *real* signal processing for Bluetooth mode. The resulting channel selection system is divided into two sections, labelled "*USB/LSB selection*" and "*bandpass filter section*" (see figure 3). The *USB/LSB selection* section includes two anti-alias lowpass filters (LPF_I, LPF_Q) of 16 taps each, to be implemented in polyphase. The Hilbert transformer (*Hb*) is also assumed to be of minimal filter length. It requires at least 50 taps to sufficiently attenuate a +40 dB stronger interferer with carrier frequency $f_{a,3} = -f_c$. This is due to pass-band ripple constraints discussed in [7]. The largest remaining bottlenecks are *BPF1* and *BPF2*, of which *BPF1* is the most critical. This is of course due to the facts that it has a variable nature¹ and that it cannot be implemented in polyphase (as there is no subsequent decimation). Thus, the *USB/LSB selection* section will remain unchanged in the following experiments, while the bandpass filter section is analyzed.

¹The filter coefficients must be updated every time the input signal hops to another frequency (refer to [8] for the hopping sequence).

A. Analysis approach

First, the bandpass filter section will be reduced to a simplified study model. Then, a step-by-step approach is chosen to track the *BER* contributions of the input signals and system components. The knowledge gained from this model will then be used to analyze the original model. There are four *worst-case* input signals (shown in figures 5(a-d)) that must be processed by the receiver and the maximum allowable *BER* of each test is $1 \cdot 10^{-3}$.

B. Bandpass filter section analysis

The bandpass filter section will be analyzed as follows: First, the section is removed entirely to find the BER_{Floor} that is imposed by the remaining receiver components and input signals of figure 6(a). This is done in experiment 1. Then, in experiment 2, one bandpass filter (*BPF*) is introduced to the system (as shown in figure 6(b)).

For each experiment, 4 input signal constellations are used to quantify the *BER* contributions of *ISI*, *ACI* and *Noise* separately. The inputs are labelled *A – D* and defined as follows:

A = *SOI* with $f_c = 2.5$ MHz

B = Signal A + bandlimited white noise (SNR 17 dB)

C = Signal A + adjacent channel interferer

D = Signal C + bandlimited white noise (SNR 17 dB)

The bandlimited white noise is added in the analog front-end (figure 1), containing a 7th order Butterworth lowpass filter with a cut-off frequency ≈ 10 MHz. In experiments 1 and 2, the (white noise only) signal to noise ratio is chosen to be 17 dB². For the Bluetooth reference tests (as described in sections II-A and IV-C) a more realistic value of 37 dB (thermal noise) is used. The *bandpass filter section* configuration in combination with the input signals yields tests denoted by test *1A*, test *2B* etc.

In experiment 2, two filter parameters will be changed: the passband width B_p and transition band width B_t (as defined in figure 7). The bandpass filter used in this experiment is an equiripple FIR, designed using the *Remez Exchange* [6] algorithm. The common parameters for the filter are listed in table I. Note that the filter order follows from pass- and stopband characteristics defined by B_p and B_t . The ranges are $B_p \in [0.4 \dots 1.1]$ MHz and $B_t \in [0.2, 0.4, 0.6]$ MHz. The filter length reduces quickly by increasing B_t (as shown in the table).

²This value is chosen to increase the *BER* and thus the reliability of the *BER* calculations

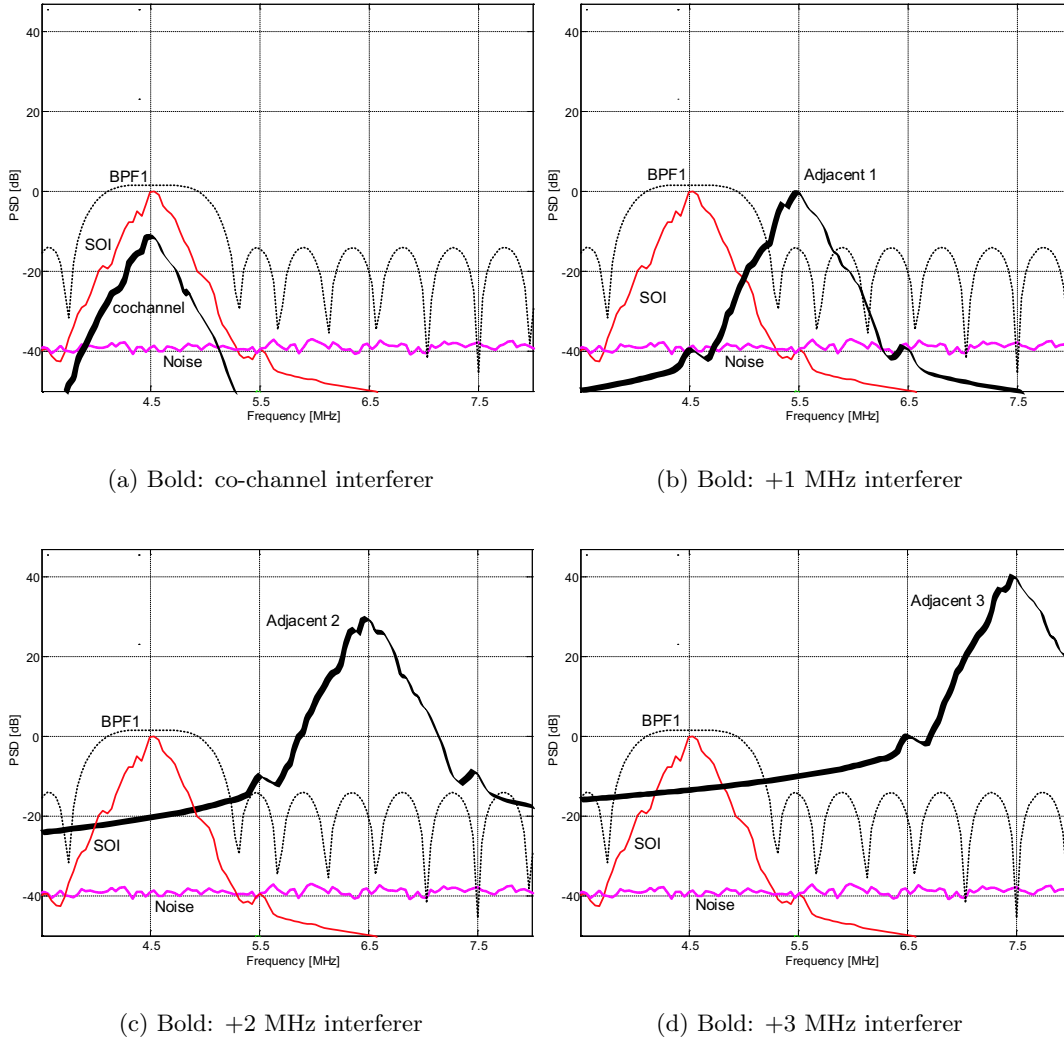


Fig. 5

TRANSFER FUNCTION OF $BPF1$ AND ITS INCOMING SIGNAL $d[n']$, FOR 4 SPECIFIED EXPERIMENTS

Parameter	Value
Type	FIR
Design method	Remez (equiripple)
Operating rate [MSPS]	20
Pass-band ripple [dB]	1
B_t [MHz]	[0.2, 0.4, 0.6]
A_s [dB]	[-23, -24, -23]
Filter order	[114, 57, 39]

TABLE I

PROTOTYPE CHANNEL SELECTION FIR FILTER

IV. EXPERIMENTS

The resulting BER of each experiment is calculated and analyzed to quantify the contributions of

BER_{ISI} , BER_{ACI} and BER_{Noise} and their dependence on the filter parameters.

A. Experiment 1

As is to be expected, without noise or interference the total BER of test 1A ($BER_{Total,1A}$) is equal to $BER_{Floor} = 0$.

$$BER_{Total,1A} = BER_{Floor,1A} = 0 \quad (1)$$

By adding noise to the input, the total bit error rate is increased by BER_{Noise} . The relation now becomes:

$$BER_{Total,1B} = BER_{Floor,1A} + BER_{Noise,1B} \quad (2)$$

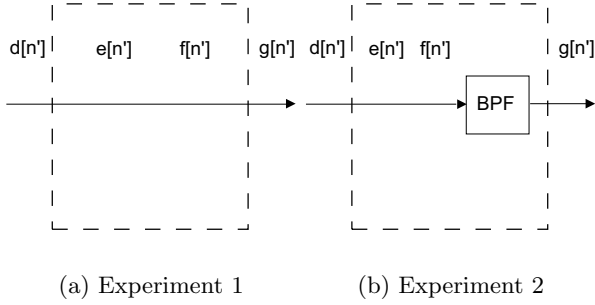


Fig. 6

BANDPASS FILTER SECTION FOR STUDY MODELS

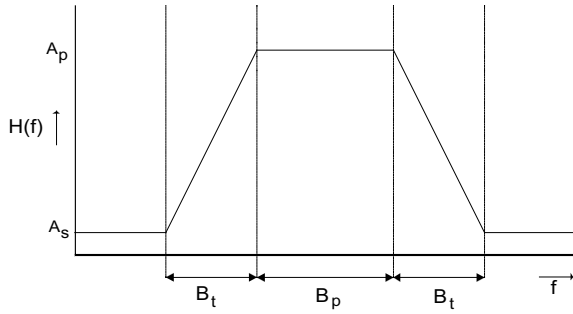


Fig. 7

SCHEMATIC TRANSFER FUNCTION OF A BANDPASS FILTER

The result of the test is a $BER_{Total,1B} = BER_{Noise,1B} \approx 0.37$ (remember that $SNR_{Noise} = 17$ dB). To find the influence of adjacent channel interference to the total BER test $1C$ is done. The expected relations are shown in eq. 3:

$$BER_{Total,1C} = BER_{Floor,1A} + BER_{ACI,1C} \quad (3)$$

The result of this test is $BER_{Total,1C} = BER_{ACI,1C} \approx 0.50$. Thus, without a filter the adjacent carrier destroys the ability to correctly receive a bit. The final test $1D$ was formulated to find other factors or correlations influencing $BER_{Total,1}$ that are not in eqs. 1-3. Unfortunately, the disruption of the BER by the adjacent channel prevents this. Clearly, a BPF is required in the system.

B. Experiment 2

Now that a filter is added to the system, BER_{ACI} must be sufficiently reduced. By reducing too much, BER_{ISI} is added to the equation. The relations that are expected to apply in test $2A$ are shown in eq. 4:

$$BER_{Total,2A} = BER_{ISI,2A} \quad (4)$$

The resulting signal has severe ISI for narrow filters, but without added noise or interference the total BER remains 0 for most simulations. This is illustrated in figure 8(a) where $\Delta A_{0,1}$ is *nearly* zero, but not quite. Thus, $BER_{Total,2B}$ is expected to be a "lifted" version of $BER_{Total,2A}$. Its constituent contributions are shown in eq. 5:

$$BER_{Total,2B} = F_{No} \cdot BER_{Noise,1B} + F_{ISI} \cdot BER_{ISI,2A} \quad (5)$$

Here, $F_{No}(B_p, B_t)$ and $F_{ISI}(B_p, B_t)$ are assumed to be scaling functions that depend on the filter characteristics. This dependency is also assumed to hold for $F_{ACI}(B_p, B_t)$ in eq.6. The resulting BER due to ISI and noise is shown in figure 8(b). The contribution of BER_{ISI} is best shown by the $BER_{Total,2B}$ of the sharpest filter with $B_t = 0.2$ MHz. It is clear that such a narrow transition band (which is also responsible for high filter orders) should not be used with B_p values ≤ 0.7 MHz.

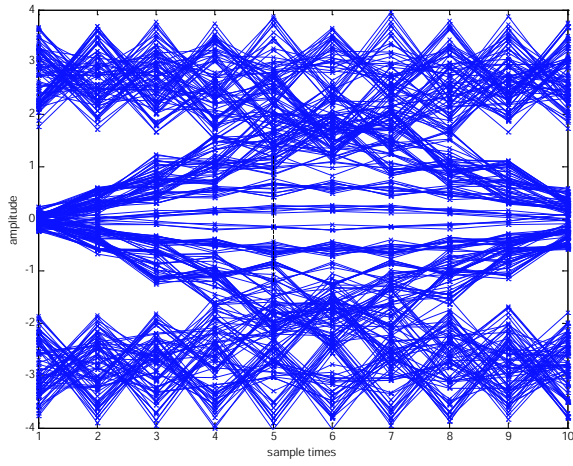
Now, to find the contribution of ACI , the noise is removed from the input signal and replaced by an adjacent carrier $f_{a,1}$. The total BER is now expected to behave as in eq.6.

$$BER_{Total,2C} = F_{ISI} \cdot BER_{ISI,2A} + F_{ACI} \cdot BER_{ACI,1C} \quad (6)$$

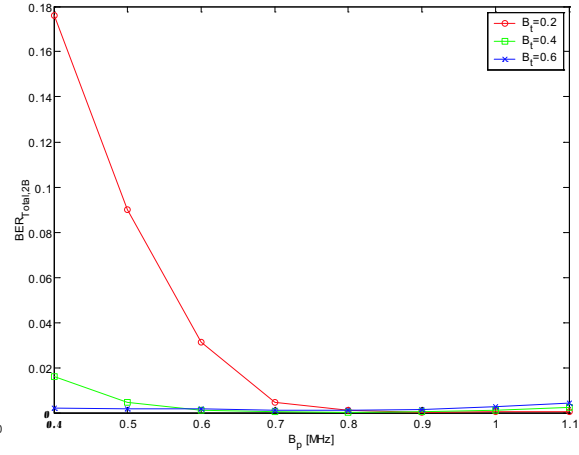
From these results, the $BER_{Total,2B}$ values will be subtracted to obtain an estimation of the ACI -only contribution. This is shown in figure 8(c). For $B_t = 0.4$ MHz, the adjacent channel interference becomes a problem for $B_p > 0.9$ MHz. The corresponding eye diagram of figure 8(d) clearly shows that when the interferer is allowed to penetrate even further into the passband, $\Delta A_{0,1}$ will be reduced to 0.

The final test $2D$ will be used to find the optimal values for B_p, B_t concerning the ACI, ISI trade-off. Furthermore, discrepancies between the assumed BER contributions and the actual simulation results can be found. The expected relations are given in eq. 7:

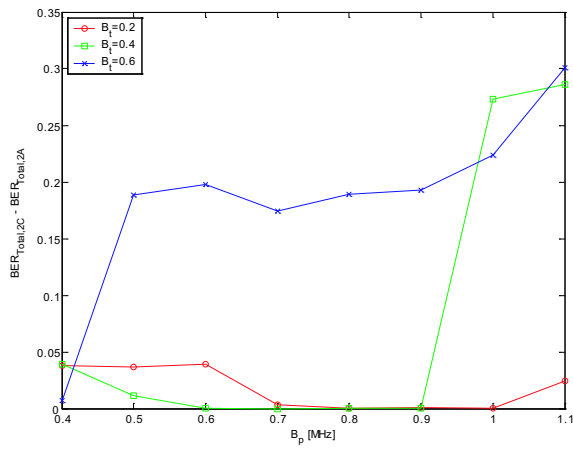
$$BER_{Total,2D} = F_{No} \cdot BER_{Noise,1B} + F_{ACI} \cdot BER_{ACI,1C} + F_{ISI} \cdot BER_{ISI,2A} \quad (7)$$



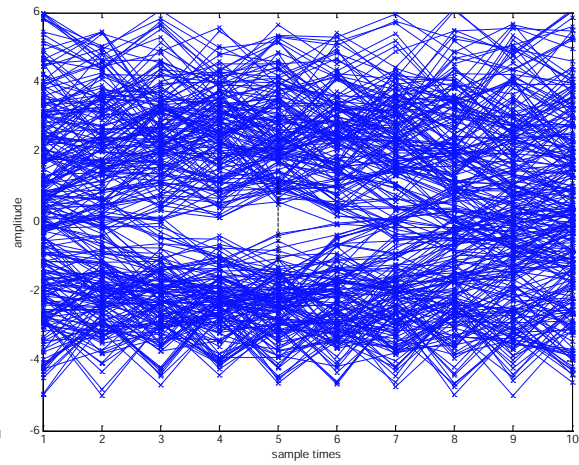
(a) ISI-only eye diagram ($B_p = 0.6, B_t = 0.2$)



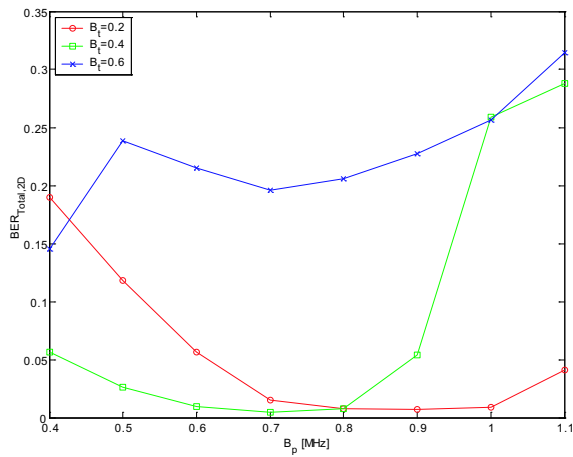
(b) BER (ISI and Noise)



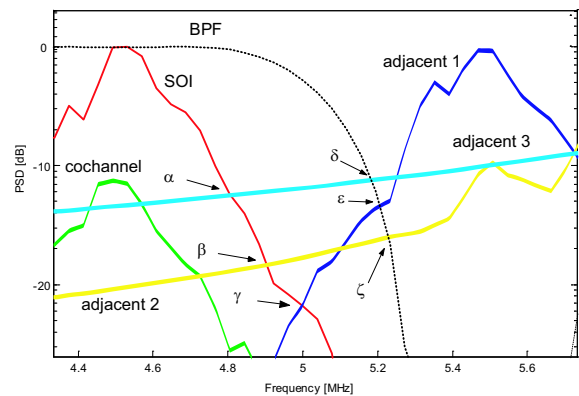
(c) BER (ACI)



(d) ACI-only eye diagram ($B_p = 0.9, B_t = 0.4$)



(e) Total



(f) Critical points

Fig. 8
EXPERIMENT 2 RESULTS

The optimal passband width is thus where the *SOI* remains unaffected by the filter for higher frequencies, but restricting the adjacent channel from interfering too much. This can be illustrated by a close-up of the *SOI* and possible interferers. Disregarding the noise for a moment, figure 8(f) shows the points where adjacent interferences "enter" the *SOI* (α, β, γ). These points can be seen as the end of the passband, as interference starts there. By choosing a smaller passband, the *SOI* is attenuated unnecessarily. B_t must then be chosen in such a way that it does not attenuate the outer lobes of the *SOI* too much, but sufficiently reduces adjacent channel interference (denoted by the points δ, ϵ, ζ). The results of this trade-off for the current input signals are shown in figure 8(e). The optimal *BPF* for these input signals is configured using $B_p = 0.7$ MHz and $B_t = 0.4$ MHz. This filter yields the minimal *BER*. A filter with $B_t = 0.6$ MHz is shown to perform significantly worse, due to excessive adjacent channel interference.

There is a discrepancy between the sum of individual *BER* contributions and BER_{Total} of test 2D. Plotting these discrepancies for the entire range shows that they are within 10% for $B_p = 0.6$ to 0.8 and all B_t . Thus, strong correlations exist between F_{ISI}, F_{ACI} and F_{Noise} in the regions where either *ISI* or *ACI* are dominant. This can be explained by the eye diagrams shown in figures 8(a) and (d). Obviously, when filter characteristics reduce the open-ness of the eye such that the noise amplitude is equal to $\Delta A_{0,1}$, it's influence is much more severe.

C. Original system

Based on the optimal filter parameters found in the previous section ($B_p = 0.7, B_t = 0.4$ MHz), the optimal bandpass filter response can be derived (as shown in figure 9(a)).

The original system (figure 3) contains two bandpass filters and must resist even stronger interferences (e.g. $f_{a,3}$, section II-A) so the combined stop-band attenuation must be ≈ 40 dB more. By optimizing for computational load, the filter length of *BPF1* is reduced (indirectly reducing *ISI*). Therefore *BPF2* is increased in length to compensate for *ACI*-induced bit errors. The *BPF2* filter type is changed to a Hamming window (FIR) filter [6] to increase stop-band attenuation (by reducing constraints on B_p and B_t). The filter responses of *BPF1* and *BPF2* are shown in figure 9(b). Their combined filter response compared to the optimal filter found is shown in 9(c). The cur-

Name	BPF1	BPF2
Type	FIR	FIR
Order	45	50
Method	Remez	Hamming
B_p [Hz]	0.6	0.1
B_t [Hz]	0.4	1.3
A_s [dB]	17	62

TABLE II
BPF1 AND BPF2 PARAMETERS

rent configuration passes all tests, and its parameters are shown in table II³

V. CONCLUSIONS

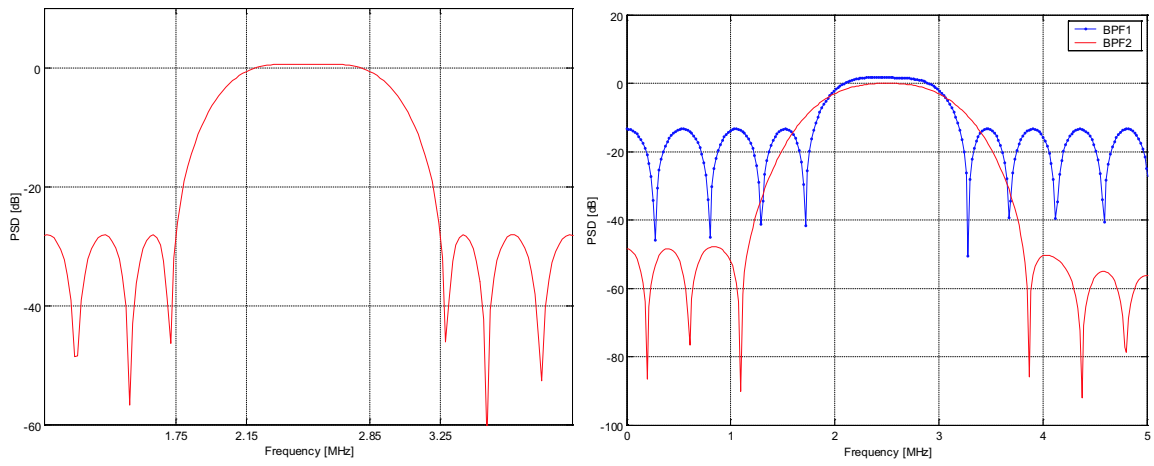
Experiment 1 has clearly proven the need for channel selection filters in case of adjacent carrier interference and high noise levels. During experiment 2 it became apparent that BER_{ACI} and BER_{ISI} behave as expected and that a clear optimum can be found between the two. The influence of the noise level to the total *BER* was shown to be extra strong in the regions where *ISI* and *ACI* are strong as well. The optimal filter parameters found in the previous section were used as guidelines for the original channel selection system. By trading off filter coefficients and *ACI* in *BPF1* (thus, the constraints on *BPF1* were relaxed), *BPF2* was used to compensate. To reduce this (extra) *ACI* contribution, a filter design method with more stopband attenuation was chosen.

REFERENCES

- [1] V.J. Arkesteijn, E.A.M. Klumperink, and B. Nauta. An analogue front-end test-bed for software defined radio. *MMSA*, 2002. Accepted for publication.
- [2] F.W. Hoeksema, R. Schiphorst, and C.H. Slump. Specification for digital channel selection filters in a bluetooth capable hiperlan/2 receiver. *2nd Karlsruhe Workshop on Software Radios*, pages 41–49, March 2002.
- [3] T.S. Rappaport. *Wireless communications*. Prentice Hall, 1996.
- [4] R. Schiphorst, F.W. Hoeksema, and V.J. Arkesteijn. The bluetooth-hiperlan/2 sdr receiver project. <http://nt5.e1.utwente.nl/sdr/>, 2002.
- [5] R. Schiphorst, F.W. Hoeksema, and C.H. Slump. Bluetooth demodulation algorithms and their performance. *2nd Karlsruhe Workshop on Software Radios*, pages 99–106, March 2002.
- [6] P.P. Vaidyanathan. *Multirate Systems and filter banks*. Prentice Hall, 1993.

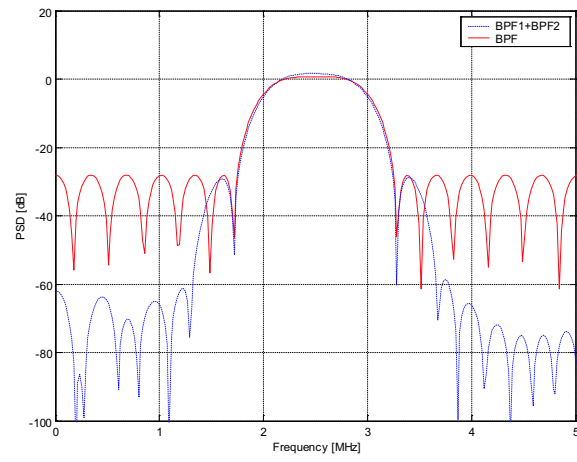
³Note that B_p, B_t could not be used directly as design parameters for *BPF2*. It was designed by cut-off frequencies 1.85 and 3.15 MHz.

- [7] L.C. van Mourik. Design & implementation of digital channel selection filters for a combined bluetooth and hiperlan/2 receiver. M.Sc. Thesis (EL-SAS-033N02), August 2002.
- [8] Various. Specification of the bluetooth system. Specification 1.1, 2 2001.



(a) Optimal BPF

(b) $BPF1$ and $BPF2$



(c) $BPF1 + BPF2$ vs optimal BPF

Fig. 9
FILTER TRANSFER FUNCTIONS